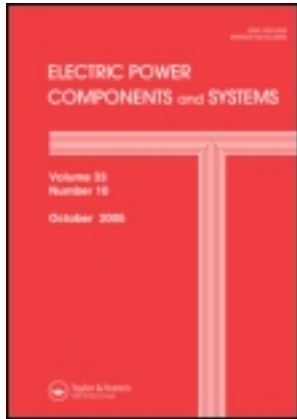


This article was downloaded by: [201.116.38.18]

On: 09 January 2013, At: 07:42

Publisher: Taylor & Francis

Informa Ltd Registered in England and Wales Registered Number: 1072954 Registered office: Mortimer House, 37-41 Mortimer Street, London W1T 3JH, UK



Electric Power Components and Systems

Publication details, including instructions for authors and subscription information:

<http://www.tandfonline.com/loi/uemp20>

Power System Stabilizer and Secondary Voltage Regulator Tuning for Multi-machine Power Systems

Ruben Tapia^a, Omar Aguilar^a, Hertwin Minor^a & Cesar Santiago^a

^a Engineering Department, Universidad Politécnica de Tulancingo, Huapalcalco, Hidalgo, México

Version of record first published: 09 Nov 2012.

To cite this article: Ruben Tapia , Omar Aguilar , Hertwin Minor & Cesar Santiago (2012): Power System Stabilizer and Secondary Voltage Regulator Tuning for Multi-machine Power Systems, Electric Power Components and Systems, 40:16, 1751-1767

To link to this article: <http://dx.doi.org/10.1080/15325008.2012.722582>

PLEASE SCROLL DOWN FOR ARTICLE

Full terms and conditions of use: <http://www.tandfonline.com/page/terms-and-conditions>

This article may be used for research, teaching, and private study purposes. Any substantial or systematic reproduction, redistribution, reselling, loan, sub-licensing, systematic supply, or distribution in any form to anyone is expressly forbidden.

The publisher does not give any warranty express or implied or make any representation that the contents will be complete or accurate or up to date. The accuracy of any instructions, formulae, and drug doses should be independently verified with primary sources. The publisher shall not be liable for any loss, actions, claims, proceedings, demand, or costs or damages whatsoever or howsoever caused arising directly or indirectly in connection with or arising out of the use of this material.

Power System Stabilizer and Secondary Voltage Regulator Tuning for Multi-machine Power Systems

RUBEN TAPIA,¹ OMAR AGUILAR,¹ HERTWIN MINOR,¹
and CESAR SANTIAGO¹

¹Engineering Department, Universidad Politécnica de Tulancingo, Huapalcalco, Hidalgo, México

Abstract *This article aims to present the performance of a B-spline neural network scheme for tuning both the reactive power provision controller from synchronous machines and power system stabilizers in multi-machine power systems. The B-spline neural network is an efficient tool to implement the adaptive control voltage and power system stabilizer coordination, with the possibility of carrying out this task on-line, taking into account the systems' non-linearities. One of the main tasks within this context is to estimate the best power system stabilizer's parameters and adjust the proportional-integral parameters for reactive power provision. In this article, this is solved by a neural network algorithm. The applicability of the proposal is demonstrated by simulation on two test systems. Results show that the proposed coordination scheme is comparable to that obtained by a conventional design, without requiring a strict model analysis.*

Keywords automatic voltage regulator, controller's coordination, multi-machine systems, oscillation mode stabilization

1. Introduction

Modern electrical power systems may be subjected to stress conditions due to the continuous growth in load. In order for consumers to receive reliable electrical power, the system's operators must ensure that bus voltages are kept within allowable limits. Power transfer from generating plants to consumption centers affects the load bus voltages; therefore, it may be necessary to add elements into the network to provide safer operation [1, 2].

In several countries the transmission system's voltage control practice is currently performed manually. This conventional way of addressing the voltage control problems often exhibits unsatisfactory performances, such as [3] (i) reactive power generation, (ii) high side voltage controls, and (iii) switching control of capacitors banks or shunt reactors.

Received 10 February 2012; accepted 6 August 2012.

Address correspondence to Ruben Tapia, Universidad Politecnica de Tulancingo, Ingenierias 100, Col. Huapalcalco, Tulancingo, Hidalgo, 43629, Mexico. E-mail: rtapia@gdl.cinvestav.mx

Another problem in power system operation is related to the small-signal oscillatory instability caused by insufficient natural damping in the system. A variety of controllers have been developed to enhance the damping of power oscillations [4–6]. The main task of these controllers is to achieve the most effective damping, especially for the electromechanical modes.

A practical power system stabilizer (PSS) must be robust over a wide range of operating conditions and capable of damping the oscillation modes. From this perspective, the conventional single-input PSS design approach based on a single-machine infinite-bus (SMIB) linearized model around one operating condition exhibits some deficiencies. (i) There are uncertainties in the linearized model resulting from the variation in the operating configuration, since the linearization coefficients are derived typically at a normal operating condition. (ii) Various techniques, such as proportional-integral-derivative (PID), artificial neural network (ANN), genetic algorithm (GA) fuzzy, hybrid neuro-fuzzy, adaptive fuzzy logic, simulated annealing, pole-shifting, etc., have been tested to achieve tuning under various operating conditions for the single-input PSS. But even after that, the single-input PSS lacks robustness in a multi-machine power system.

In a PSS, the electrical power P_e and the rotor angular speed variation $\Delta\omega$ are calculated from the generator's voltage and current measured values. In stationary operation, deviations in the electrical power are used to evaluate the optimum stabilizing signal in terms of amplitude and phase relationship by means of a lead/lag filter.

Currently, many plants employ conventional lead-lag structure PSSs, due to the ease of on-line tuning and reliability. Over the last two decades, various PSS parameters' tuning schemes have been developed and applied to solve the problem of dynamic instability in power system. Recently, several modern control techniques have been used to design different PSSs. To increase the stabilizer's damping performance, recent research has paid attention to tuning these stabilizers simultaneously [7–16].

In [10], an improved direct feedback linearization adaptive control algorithm was developed for achieving both voltage regulation and transient stability simultaneously. This work uses a standard third-order model of a synchronous generator, which only requires information about the physically available measurements of angular speed, active power, and generator terminal voltage. In real time for an SMIB power system, the control scheme is implemented. An output feedback controller is proposed to enhance the transient stability of non-linear multi-machine power systems using a sliding-mode speed stabilizer/sliding-mode voltage regulator [15]. The control law is proved only in an electric power system (EPS) with three machines and nine buses, based on the eighth-order generator model. In [16], a multi-machine EPS with four machines and nine buses was used to assess the robustness and performance capabilities of a PSS and automatic voltage regulator (AVR) scheme. The controller proposed is based on an adaptive neuro-fuzzy inference system to enhance the transient stabilization, but the secondary voltage regulation has not been addressed.

Therefore, the PSS and secondary voltage regulation used in an EPS for increasing stability margins in real-time operation is an important topic that must be extended considering real system conditions. In most of the literature, the controllers' parameters are adjusted separately [10], and both secondary voltage regulation and system stability enhancement is difficult to attain simultaneously. Otherwise, the controllers are calculated according to approximately linearized power systems models, but the system dynamic performance may deteriorate when the operating point changes to some extent.

The PSS parameters' tuning has been approached by two major strategies, sequential tuning and simultaneous tuning. In order to obtain the set of optimal PSS parameters under

various operating conditions, the tuning and testing of PSS parameters must be repeated under various system operating conditions. Therefore, if the sequential tuning method is applied to tune PSS parameters, the parameters tuning will become more complicated, and the result may not be a local or global optimal solution. On the other hand, in the case that the simultaneous tuning method is employed for tuning the PSS parameters, which can simultaneously relocate and coordinate the eigenvalues for various oscillating modes under different operating conditions, the set of PSS parameters can be quite close to the globally optimal solution. However, the drawback of the simultaneous tuning method is the long computation time required for large power systems.

The simultaneous tuning of PSS parameters is usually formulated as a very large-scale non-linear non-differentiable optimization problem. This kind of optimization problem is very hard to solve using conventional differentiable optimization algorithms. That is, the problem of the PSS design is a multi-modal optimization problem (*i.e.*, more than one local optimum exists). Hence, conventional optimization techniques may be not suitable for such a problem.

The modern power systems represent a huge operational challenge. They exhibit highly complex topology and varied structural components. Usually, decentralized control devices are employed, which provides local control to different power grid equipment, such as PSSs, AVRs, flexible AC transmission systems (FACTS) devices, etc. These control agents have helped to alleviate voltage, frequency, and angular problems and to mitigate inter-area oscillations. However, the new control elements connected to the system must be able to positively interact with the previously installed controllers. Thus, they must be coordinated to obtain a satisfactory performance.

In this article, a B-spline neural network (B-SNN) is employed two main tasks: one for the secondary voltage regulator (SVR) and one for PSS coordination, taking care of a key feature—the proposed controller must be able to enhance the PSS's performance for damping purposes. The strategy is proposed to update conventional PSSs currently operating in power systems that were tuned long ago. The main idea is basically to re-tune the control gains through an on-line procedure, which involves a few measurements. After that, the same controllers' devices may continue working properly under different operating conditions and topologies. Results show that this idea works adequately, independently of the studied power system.

2. PSS Design

2.1. Power System Model

In this article, two power systems available in the open research are employed in order to exemplify the proposition. The development of systematic methodologies for PSS tuning is a problem that requires special attention. Once it is determined that a system requires effective damping, especially for the electromechanical modes, the fundamental problem is to find the best control parameters (static or dynamic). The deficiency of damping can be solved by means of PSSs.

However, it is necessary to have some type of coordination algorithm. On the other hand, for an SVR, the proportional-integral (PI) parameters values are required to obtain a good reactive power provision for each machine. In this article, an on-line strategy is applied to re-tune PSSs and SVR control parameters in order to adapt them to new circumstances. The fourth-order dynamic model is utilized for generators, including a

static excitation system [2]. The set of equations for each generator becomes:

$$\frac{d\delta}{dt} = \omega - \omega_0, \quad (1)$$

$$\frac{d\omega}{dt} = \frac{1}{M}(T_m - T_e - D\omega), \quad (2)$$

$$\frac{dE'_d}{dt} = \frac{1}{T'_{d0}}[-E'_d + (x_q - x'_q)i_q], \quad (3)$$

$$\frac{dE'_q}{dt} = \frac{1}{T'_{d0}}[E_{fd} - E'_q - (x_d - x'_d)i_d], \quad (4)$$

$$\frac{dE_{fd}}{dt} = \frac{1}{T_A}[-E_{fd} + K_A(V_{ref} - V_t + V_s)], \quad (5)$$

where

δ (rad) and ω (rad/s) represent the rotor angular position and angular velocity,

E'_d (p.u.) and E'_q (p.u.) are the internal transient voltages of the synchronous generator,

E_{fd} (p.u.) is the excitation voltage,

i_d (p.u.) and i_q (p.u.) are the d - and q -axis currents,

T'_{d0} (sec) and T'_{q0} (sec) are the d and q open-circuit transient time constants,

x'_d (p.u.) and x'_q (p.u.) are the d and q transient reactances,

x_d (p.u.) and x_q (p.u.) are the d and q synchronous reactances,

T_m (p.u.) and T_e (p.u.) are the mechanical and electromagnetic nominal torque,

M is the inertia constant,

D is the damping factor,

K_A and T_A (sec) are the system excitation gain and time constant,

V_{ref} is the reference voltage,

V_t is the terminal voltage magnitude, and

V_s is the PSS's output signal.

2.2. PSS Model

The interaction between stabilizers may increase or decrease the damping of certain oscillation rotor modes. To have a better performance in this respect, proper coordination is required of all control devices used in the network, while also ensuring robustness under different operating conditions.

A typical static excitation system has V_s as input, which is the modulation signal from the PSS. The structure of a conventional PSS connected to the k th machine consists of a gain, a washout unit, units of phase compensation, and an output limiter, as shown in Figure 1. The washout unit is used to prevent changes of state of the input signal by changing the voltage at terminals. In this article, both parameters—the gain k and the time constant T —are updated on-line to attain a proper performance under different operating conditions, without restructuring power stations. The use of the angular velocity deviation $\Delta\omega_i$ is assumed as the PSS's input (Figure 1).

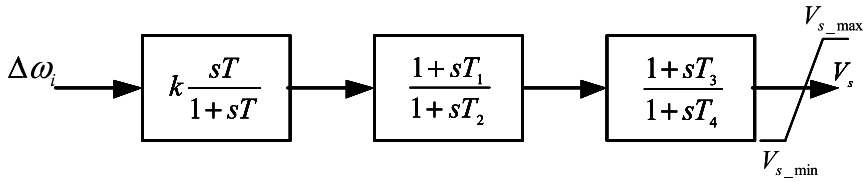


Figure 1. PSS block diagram.

To simplify the procedure, it is assumed that $T_1 = T_3$ and $T_2 = T_4$. These parameters remain in their original values, but, of course, they could be adapted.

2.3. SVR Scheme

This article employs the concept of secondary voltage control proposed in [17]. The proposition allows regulating the VAR provision for each generator according to its rating. This strategy helps to accomplish an efficient VAR injection into the network, handling the reactive flows depending on the load variation. Likewise, the pilot nodes' regulation improves the voltage profile around critical areas. PI controllers will be utilized: one for each generator plus a central controller, which estimates the reactive power that each generator delivers (Figure 2). The required measurements are (a) reactive power coming from each generator (b) generators' terminal voltage, and (c) the pilot node voltage magnitude. This article proposes the use of adaptive PI controllers to maintain the reactive power control in each generator in order to avoid stressed conditions under load variations throughout the day.

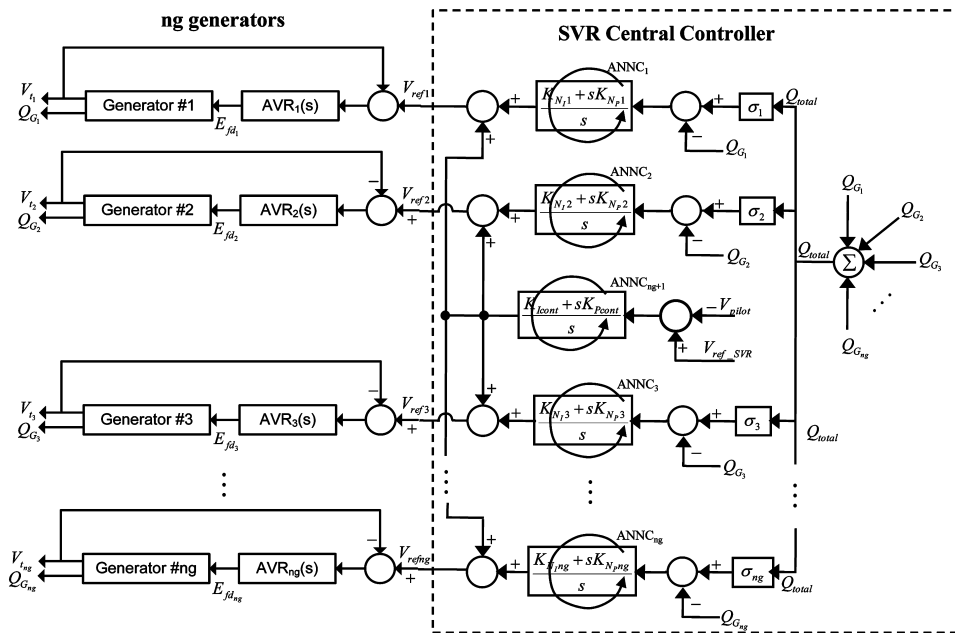


Figure 2. SVR scheme for multi-machine power system.

Downloaded by [201.116.38.18] at 07:42 09 January 2013

This can be achieved adding a B-SNN to update K_P and K_I gains in the $ng + 1$ PI controllers (Figure 2), where each PI transfer function is given by

$$\frac{U(s)}{E(s)} = \frac{K_I + K_P s}{s}. \quad (6)$$

Thus, K_P and K_I are updated from a B-SNN at every sampled time. With this purpose, $2(ng + 1)$ ANNs are assembled in the control scheme. In Figure 2, $\sigma_1, \sigma_2, \dots, \sigma_{ng}$ are weighting factors to share the total reactive power; they are selected according to the generator's rating. Thus, the appropriate reactive power regulation will provide enough reserve under stressed conditions.

3. Proposition

The major advantages of the ANNs are the controller's design simplicity, their compromise between the complexity of a conventional non-linear controller, and its performance. The B-SNNs are a particular case of neural networks that allows the control and modeling of systems adaptively, with the option of carrying out such tasks on-line and taking into account the power grid non-linearities.

3.1. Neural Network Structure

A B-spline function is a piecewise polynomial mapping that is formed from a linear combination of basis functions, and the multivariate basis functions are defined on a lattice [18]. The on-line B-spline associative memory network (AMN) adjusts its weights iteratively in an attempt to reproduce a particular function, whereas an off-line or batch B-spline algorithm typically generates the coefficients by matrix inversion or using conjugate gradient. B-spline AMNs adjust their (linear) weight vector, generally using instantaneous least mean square (LMS)-type algorithms, in order to realize a particular mapping, modifying the strength with which a particular basis function contributes to the network output.

Through B-SNNs, there is the possibility to bound the input space by the basis functions definition. Generally, only a fixed number of basis functions participate in the network's output. Therefore, not all the weights have to be calculated each sample time, thus reducing the computational effort and time. In general, the B-SNN's output can be described by [18]

$$y = \mathbf{a}\mathbf{w}, \quad (7)$$

$$\mathbf{w} = [w_1 \quad w_2 \quad \dots \quad w_p]^T, \quad \mathbf{a} = [a_1 \quad a_2 \quad \dots \quad a_p], \quad (8)$$

where w_i and a_i are the i th weight and the i th B-SNN basis function output, respectively; p is the number of weighting factors. i refers to a sub-index that can take values from 1 to p (vector dimension), and p represents the number of weighting factors, which depends on a particular application. In this case, only one weighting factor was used to each ANN (Figure 3). It allows diminishing of the computational effort with good system response.

This article proposes that k and T be adapted through one B-SNN, respectively (Figure 1); also, K_P and K_I for each SVR scheme are calculated (Figure 2). The

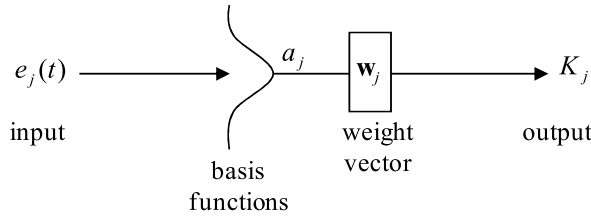


Figure 3. Proposed B-SNN for adapting PSS and SVR control parameters.

angular velocity deviation from its nominal value e_x is the input signal to adapt gain k , while the generator's active power deviation from its nominal capacity e_y is the input signal to adapt the time constant T . In the other case, for the SVR scheme, the input signal to calculate K_p is the reactive power difference e_z from the σ factor. Finally, the input variable to obtain the K_I value is the same e_x . Such an election is made based on the close relationship between active power and velocity with respect to the damping. Then the dynamic control parameters for a multi-machine system can be described as follows:

$$k = NN_j(e_x, w_j), \quad (9)$$

$$T = NN_j(e_y, w_j), \quad (10)$$

$$K_p = NN_m(e_z, w_m), \quad (11)$$

$$K_I = NN_m(e_x, w_m), \quad (12)$$

where NN_j denotes the B-spline network that is used to calculate k and T , and w_j is the corresponding weighting factor ($j = 1, 2, \dots$, number of PSSs $[n_{ps}]$). Also, NN_m denotes the B-spline network that is used to calculate K_p and K_I , and w_m is the corresponding weighting factor ($m = 1, 2, \dots$, number of generators $[n_g]$ plus one). Figure 3 depicts a scheme of the proposed B-SNN.

In order to introduce an adaptive strategy, one neural network with $n_{ps} + n_g + 1$ as the number of input signals with the same number of output signals is used to calculate the best control parameters for both PSS and SVR schemes. The appropriate design requires the following *a priori* information: the bounded values of e_x , e_y , and e_z and the size, shape, and overlap definition of the basis function. Such information allows the bounding the B-SNN input and the enhancement of the convergence and stability of the instantaneous adaptive rule [18]. Likewise, with this information, the B-SNN estimates the optimal weights' value. The neural network adaptive parameters (Eqs. (9)–(12)) are created by univariate basis functions of order 3, considering that e_x , e_y , and e_z are bounded within $[-1.5, 1.5]$ p.u.

3.2. Learning Rule

Learning in ANNs is usually achieved by minimizing the network's error, which is a measure of its performance, and is defined as the difference between the actual output vector of the network and the desired one.

On-line learning of continuous functions, mostly via gradient-based methods on a differentiable error measure, is one of the most powerful and commonly used approaches to train large layered networks in general [19] and for non-stationary tasks in particular.

In this application, the parameters' quick updating is sought. While conventional adaptive techniques are suitable to represent objects with slowly changing parameters, they can hardly handle complex systems with multiple operating modes. The instantaneous training rules provide an alternative so that the weights are continually updated and reach the convergence to the optimal values. Also, conventional nets sometimes do not converge or their training takes too much time [19–21]. In this article, the neural network is trained on-line using the following error correction instantaneous learning rule [19]:

$$w_i(t) = w_i(t-1) + \frac{\eta e_i(t)}{\|\mathbf{a}(t)\|_2^2} a_i(t), \quad (13)$$

where η is the learning rate, and $e_i(t)$ is the instantaneous output error.

With respect to the learning rate, it takes one point within the interval $[0, 2]$ as an initial value for stability purposes [18]. This value is adjusted by trial and error. If η is set close to 0, the training becomes slow. On the contrary, if this value is large, oscillations may occur. In this application, it settles down in 0.0057 for k , 0.00136 for T , 0.00135 for K_P , and 0.00025 for K_I . It is proposed that during the actualization procedure, a dead band is included to improve the learning rule convergence. The weighting factors are not updated if the error has a value below 3%:

$$w_i(t) = \begin{cases} w_i(t-1) + \frac{\eta e_i(t)}{\|\mathbf{a}(t)\|_2^2} a_i(t) & \text{if } |e_i| > 0.003 \\ w_i(t-1) & \text{otherwise} \end{cases}. \quad (14)$$

This learning rule has been elected as an alternative to those that use, for instance, Newton's algorithms for updating the weights [21, 22] that require Hessian and Jacobian matrix evaluation. Regarding the weights' updating, Eq. (13) should be applied for each input–output pair in each sample time; the updating occurs if the error is different from zero, which is the reason that the weights converge to optimal values [18].

Thus, the proposition consists fundamentally of establishing its structure (the definition of basis functions) and the value of the learning rate. Regarding the weights' updating, Eq. (13) should be applied for each input–output pair in each sample time; updating occurs if the error is different from zero. With respect to the learning rate, it takes as an initial point one value inside the interval $[0, 2]$ due to stability purposes [18]. This value is adjusted through trial and error; with a value close to zero, the training becomes slow. Hence, the B-SNN training process is carried out continuously on-line, while the weights' value are updated using only two feedback variables.

4. Test Results and Analysis

In order to demonstrate the feasibility of this proposition, two multi-machine power systems of open research are employed. The proposed tuning performance is exhibited. To analyze the results, simulations are developed under different scenarios: (i) with the PSS and SVR tuned by optimization [22] (static parameters), or FXPSS; (ii) with the PSS and SVR tuned by B-SNN (dynamic parameters), or ANNPSS. Several operating conditions are taken into account.

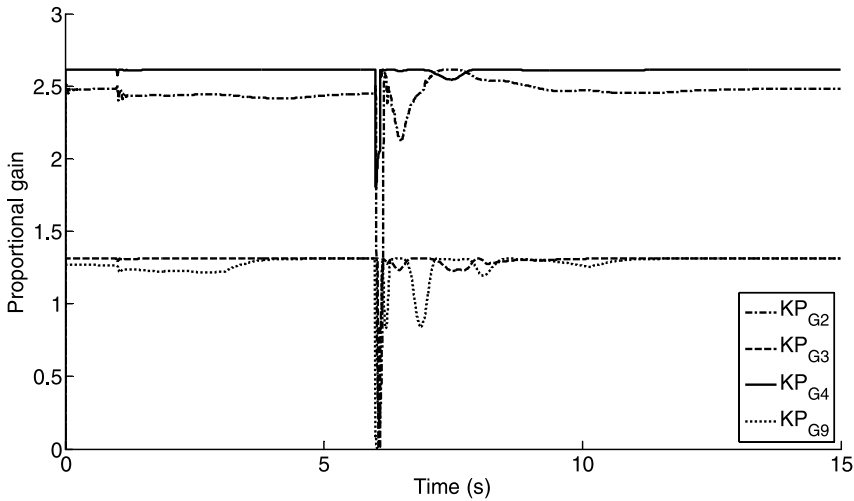


Figure 4. Proportional gain for SVR scheme, case 1.

4.1. First Analysis System

In this section the 39-bus, 10-generator test system is analyzed [23]. To examine the results, four conditions are presented. Comparisons are made with the response obtained using the PSS and SVR with fixed parameters (Figures 4–6). The PSS and SVR data are summarized in the Appendix.

The first condition shows the system’s evolution when the reactive power is decreased in 5% at $t = 1$ sec, then at $t = 6$ sec with a three-phase fault at bus 21 with duration of 86 ms; after that time, the fault is cleared. Figure 4 displays the evolution of the proportional gains for four generators. Quite similar results are exhibited for all adaptive

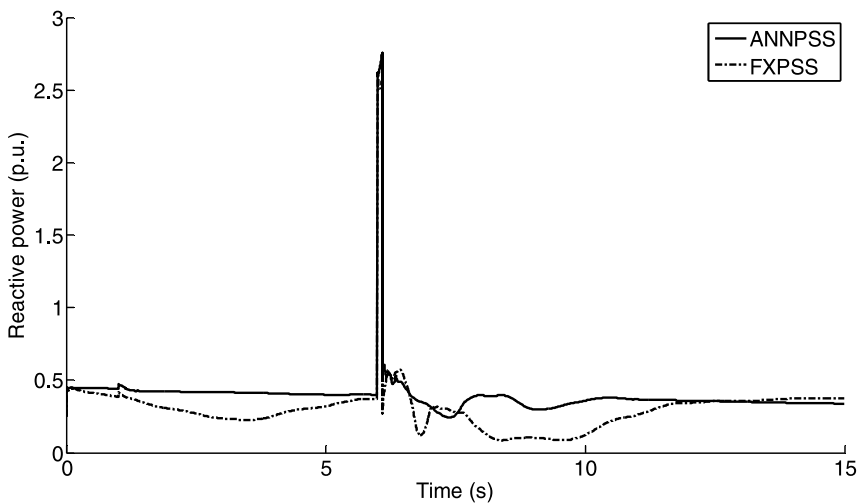


Figure 5. Reactive power Q_8 generator 8 performance, case 3.

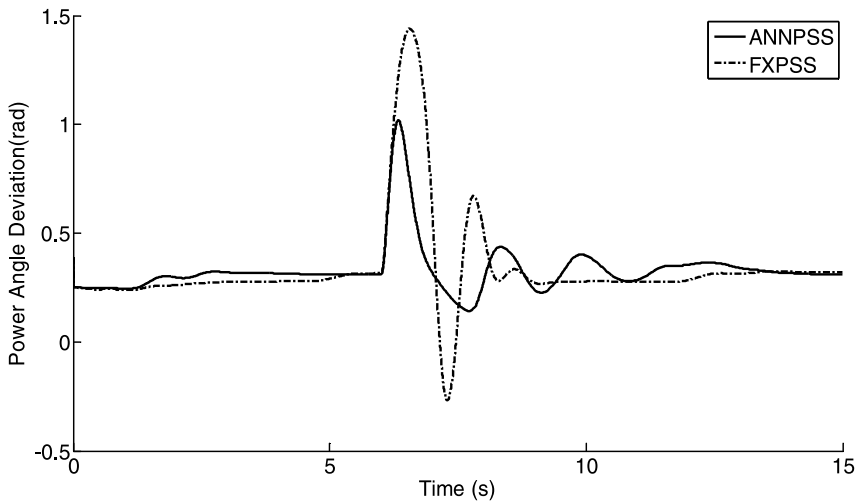


Figure 6. Power angle deviation evolution δ_{91} generator 9 performance, case 4.

parameters (PSS and SVR schemes). The initial conditions for each neural network algorithm are based on typical values for all parameters control.

The second condition illustrates the system's evolution when the reactive power is decreased in 9% at $t = 1$ sec is also under a three-phase fault in bus 24 lasting for 85 ms; after that, the fault is cleared without reconfiguration.

The third and fourth cases validate the appropriate system evolution under reactive power increased at 5 and 10%, respectively, then at $t = 6$ sec with a three-phase fault at buses 35 and 29, respectively, lasting for 85 ms; after that time, the fault is cleared. Figure 5 shows that the dynamic behavior of the reactive power at generator 8 (case 3), where the proposed scheme is better than that of the conventional PSS and SVR with fixed parameters. In this case, two perturbations are presented; in both, the reactive power response with the proposed scheme (ANNPSS) has better performance with respect to fixed parameters (FXPSS) of the SVR and PSS controllers, considering the transient- and steady-state conditions. For example, the overshoot is less than 0.1; on the other hand, with fixed parameters, it is about 0.2; the settling time is 0.2 sec with respect to 5 sec with FXPSS, in the first perturbation. For the second, to achieving the steady-state condition is about 2 sec more for fixed parameters, and the overshoot is larger, around 0.2. The steady-state values can be compared in Table 1, where it can be seen that the proposed schemes attain less error with respect to the reference in the SVR scheme. The performance of the tuning technique is in accordance with conditions 1, 2, and 3. ANNPSS exhibits very good performance, adapting itself to the new conditions. Figure 6 presents the power angle deviation in generator 9 for case 4, where the controllers' performance aids in maintaining the power system's variables within permissible limits.

Table 2 illustrates the steady-state parameters reached by the neural network for the PSS design, showing that they are updated under different operating conditions. Thus, depending on the power system topology, these parameters modify their value.

Table 1 presents the steady-state performance of reactive power contributed by each generator under the SVR algorithm. It is seen that it gets a minor total error in steady state with the proposed parameter-updating scheme on maintaining fixed parameters' values.

Table 1
Reactive power performance in steady state by neural network algorithm

Generator	Q %	Steady-state Q (p.u.)	Case 1: $t = 1 \text{ sec } Q_{out} 5\%; t = 6 \text{ sec fault at bus 21}$			Case 2: $t = 1 \text{ sec } Q_{out} 9\%; t = 6 \text{ sec fault at bus 24}$			
			Desired Q	Actual Q	ANNPSS	Actual Q	FXPSS	Desired Q	Actual Q
1	13.09	2.0709	1.967355	1.8732	1.8731	1.884519	1.7209	1.7213	
2	14.02	2.2175	2.106625	2.0185	2.0211	2.017925	1.8440	1.9226	
3	12.69	2.0069	1.906555	1.8145	1.8132	1.826279	1.6644	1.6629	
4	9.25	1.4633	1.390135	1.3200	1.3201	1.331603	1.2156	1.2155	
5	5.54	0.8762	0.83239	0.8715	0.8679	0.797342	0.8723	0.8806	
6	17.04	2.6955	2.560725	2.7384	2.7729	2.452905	2.7148	2.7303	
7	9.49	1.5015	1.426425	1.7905	1.7436	1.366365	1.8426	1.7416	
8	2.80	0.4433	0.421135	0.4144	0.4276	0.403403	0.4410	0.4620	
9	4.50	0.7111	0.675545	0.4976	0.4966	0.647101	0.4597	0.4586	
10	11.57	1.8300	1.7385	1.6575	1.6556	1.6653	1.5317	1.5244	
Total	100	15.8162	15.02539	14.9961	14.9918	14.3927	14.3071	14.3198	
% error			0.19	0.22			0.59		

Generator	Q %	Steady-state Q (p.u.)	Case 3: $t = 1 \text{ sec } Q_{in} 5\%; t = 6 \text{ sec fault at bus 35}$			Case 4: $t = 1 \text{ sec } Q_{in} 10\%; t = 6 \text{ sec fault at bus 29}$			
			Desired Q	Actual Q	ANNPSS	Actual Q	FXPSS	Desired Q	Actual Q
1	13.09	2.0709	2.174445	2.2864	2.2963	2.27799	2.4899	2.5215	
2	14.02	2.2175	2.328375	2.3126	2.3177	2.43925	2.4026	2.4788	
3	12.69	2.0069	2.107245	2.2216	2.2269	2.20759	2.5681	2.4109	
4	9.25	1.4633	1.536465	1.6057	1.6092	1.60963	1.7407	1.7625	
5	5.54	0.8762	0.92001	0.9373	0.8592	0.96382	1.1032	0.8475	
6	17.04	2.6955	2.830275	2.7800	2.8849	2.96505	2.6931	2.9281	
7	9.49	1.5015	1.576575	1.6095	1.5315	1.65165	1.3649	1.4787	
8	2.80	0.4433	0.465465	0.3388	0.3731	0.48763	0.2464	0.2099	
9	4.50	0.7111	0.746655	0.6010	0.6027	0.78221	0.7050	0.6574	
10	11.57	1.8300	1.9215	2.0213	2.0210	2.013	2.2621	2.3197	
Total	100	15.8162	16.607	16.7142	16.7224	17.3978	17.5760	17.6149	
% error			0.64	0.69			1.02		

Table 2
PSS adaptive parameters in steady state

Parameters	Case 1:	Case 2:	Case 3:	Case 4:
	$t = 1$ sec Q_{out} 5%; $t = 6$ sec fault at bus 21	$t = 1$ sec Q_{out} 9%; $t = 6$ sec fault at bus 24	$t = 1$ sec Q_{in} 5%; $t = 6$ sec fault at bus 35	$t = 1$ sec Q_{in} 10%; $t = 6$ sec fault at bus 29
k	207.1153	207.1202	207.1153	207.1153
	509.8731	509.8731	509.8731	509.8731
	491.4195	491.4214	491.4175	491.4195
	122.0566	122.0670	122.0631	122.0629
	89.3447	89.3483	89.3522	89.3511
	373.8666	373.8669	373.8679	373.8683
	719.8990	719.8984	719.8969	719.9024
	255.3865	255.3877	255.3875	255.3875
	439.0476	439.0510	439.0481	439.0456
	167.9558	167.9530	167.9558	167.9548
T	7.4919	7.4922	7.4916	7.4919
	7.4620	7.4576	7.4716	7.4898
	7.4900	7.4894	7.4918	7.4911
	7.4943	7.4935	7.4928	7.4927
	7.4932	7.4952	7.4936	7.4917
	7.5027	7.4959	7.4950	7.4910
	7.4975	7.4970	7.4955	7.4932
	7.4927	7.4921	7.4943	7.4945
	7.4894	7.4940	7.4912	7.5434
	7.4931	7.4931	7.4935	7.4917
$T_1 = T_3$		0.08		
$T_2 = T_4$		0.015		

There is a comparison of desired reactive power contribution and simulation results obtained; only in case 2 are the results different.

4.2. Second Analysis System

The New England system consists of 16 machines and 68 nodes [24]. The transient model is used for generators, and neuronal control parameters are specified in Section 3. For testing, the proposed three cases are presented: (1) three-phase fault at bus 63—after 85 ms, the system returns to pre-fault condition; (2) this case illustrates the system evolution when in $t = 1$ sec, a three-phase fault on bus 33 is simulated, lasting for 85 ms; and (3) at $t = 0.5$ sec, a three-phase fault at bus 56 is simulated, lasting for 85 ms.

Figures 7–10 depict the system behavior, where satisfactory coordinated performance can be appreciated. Figure 7 presents the angular difference evolution in generators 1, 7, 9 and 11 under condition 1. The PSS and SVR data are given in the Appendix. Figure 8 shows the dynamic behavior of nodal voltages close to the failed node response observed

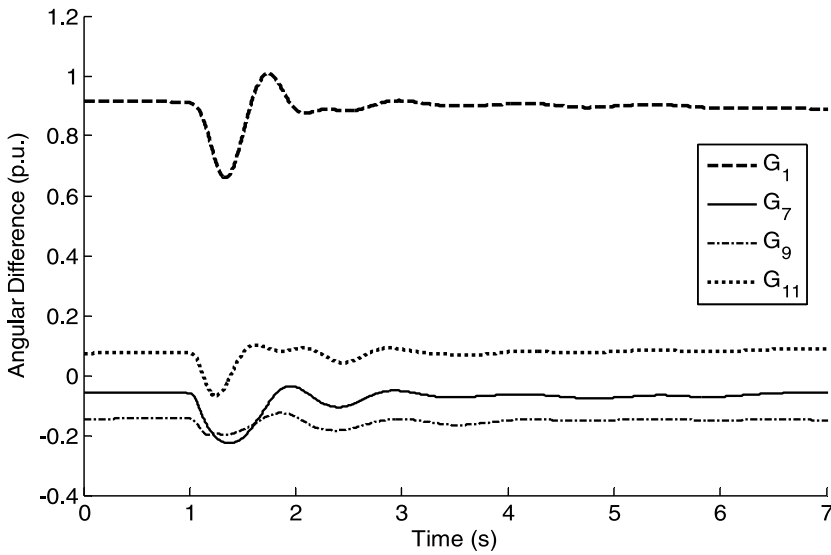


Figure 7. Angular difference performance with adaptive parameters considering machine 13 as reference, case 1.

with low oscillations and achieving steady-state values similar to pre-fault. It compares both results with ANNPSS and FXPSS; the overshoot and oscillations are larger without retuning the results with the proposal scheme.

Figure 9 depicts the dynamic performance of reactive power in generators 2, 5, 11 and 15 based on the proposed scheme, achieving the values desired by the SVR algorithm. Table 3 shows the steady-state values of generator 4 to illustrate the results obtained by

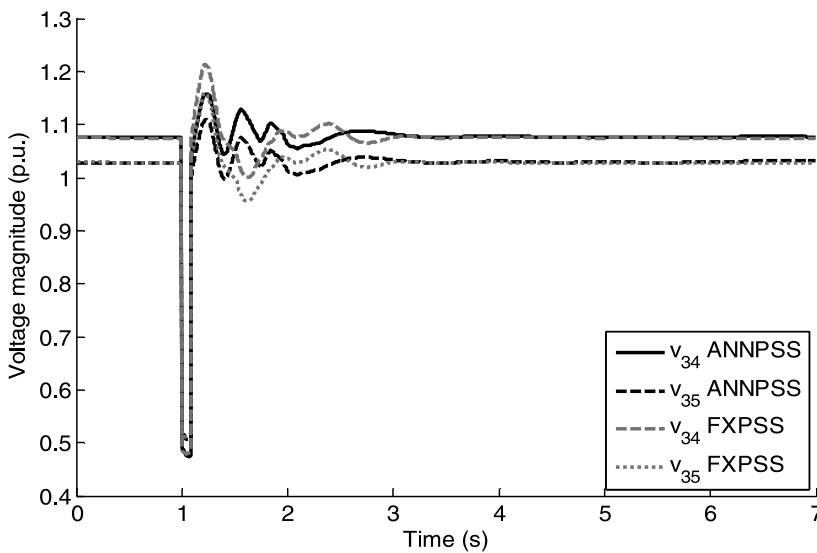


Figure 8. Voltage magnitude performance with adaptive and fixed parameters, case 2.

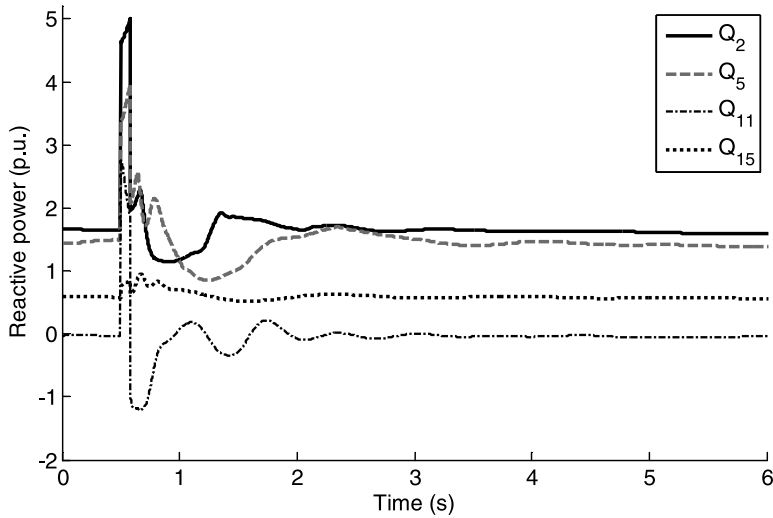


Figure 9. Reactive power performance with adaptive parameters, case 3.

tuning the PSS and SVR based on adaptive parameters, keeping all three cases very close to the desired value. Finally, Figure 10 presents the active power evolution with the proposal and considering fixed parameters. The transient response is diminished in terms of overshoot magnitude without updated parameters. The controllers' performance can be weakened in some operation conditions, as the tuning process was made previously. In large power systems, it is difficult to guarantee a suitable performance in all cases for interesting variables; this proposal can be considered a good option to overcome these shortcomings.

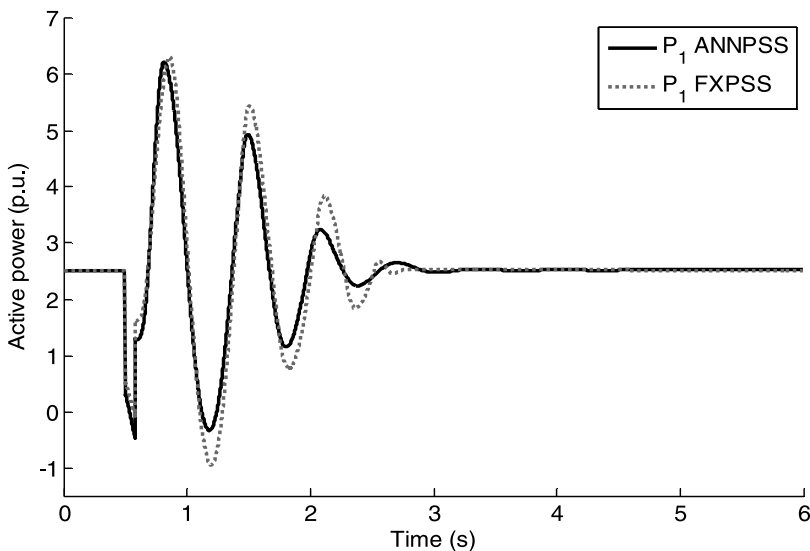


Figure 10. Active power performance with adaptive and fixed parameters, case 3.

Table 3
Reactive power in steady state

Generator	Steady state without SVR, Q	Case 1 Q	Case 2 Q	Case 3 Q
2	1.8428	1.6087	1.5599	1.5891
5	1.6234	1.4146	1.4006	1.3919
12	2.4914	2.4852	2.4261	2.5978
15	0.6718	0.5817	0.4418	0.5625

5. Conclusion

The aim of the article is to show the performance of adaptive PSS and SVR parameters as a means to enhance power system oscillations. In order to attain such purposes, a B-SNN is proposed. With this neural adaptive scheme, the possibility of implementing the on-line updating parameters has potential due to its learning ability and adaptability, robustness, simple algorithm, fast calculations, and not exclusive but inclusive nature to get a better solution under hardware constraints. This is desirable for practical hardware implementation in power stations.

Unlike the conventional technique, the B-spline ANN exhibits an adaptive behaviour, since the weights can be adapted on-line, responding to inputs and error values as they arise. Also, it can take into account non-linearities, un-modeled dynamics, and un-measurable noise. Simulations on two multi-machine power systems under different disturbances and operating conditions demonstrate the effectiveness and robustness of the proposed strategy. Dynamic and steady-state responses are analyzed.

There is a need for on-line tuning not only for PSS parameters also for SVR PI controllers. It is a convenient tool because, in practice, the electrical grid is operating; therefore, maybe only a few controller parameters must retune on-line, considering that they exhibit a low performance in some operation conditions. Besides, the proposal allows that many parameters achieve its optimal value without previous model system knowledge; only some experience about variables performance is required.

Acknowledgment

The authors thank CONACyT by support (grant 130107).

References

1. Taylor, C. W., *Power System Voltage Stability*, USA: McGraw-Hill, Chaps. 7 and 8, 1993.
2. Anderson, P. M., and Fouad, A., "Power system stability," in *Power System Control and Stability*, 2nd ed., USA: IEEE Press, Chap. 1, 2003.
3. Taylor, C. W., "Line drop compensation, high side voltage control, secondary voltage control—why not control a generator like a static var compensator?" *IEEE Summer Mtg.*, Vol. 1, pp. 307–310, 2000.
4. Kundur, P., Klein, M., Rogers, G., and Zywno, M., "Application of power system stabilizers for enhancement of overall system stability," *IEEE Trans. Power Syst.*, Vol. 4, No. 2, pp. 614–626, May 1989.

5. Gibbard, M. J., and Vowels, D. J., "Reconciliation of methods of compensation for PSSs in multimachine systems," *IEEE Trans. Power Syst.*, Vol. 19, No. 1, pp. 463–472, February 2004.
6. Qiu, W., Vittal, V., and Khammash, M., "Decentralized power system stabilizer design using linear parameter varying approach," *IEEE Trans. Power Syst.*, Vol. 19, No. 4, pp. 1951–1960, November 2004.
7. Do Bomfim, A. L. B., Taranto, G. N., and Falcao, D. M., "Simultaneous tuning of power system damping controllers using genetic algorithm," *IEEE Trans. Power Syst.*, Vol. 15, pp. 163–169, February 2000.
8. Abdel-Magic, Y. L., Abido, M. A., Al-Baiyat, S., and Mantawy, A. H., "Simultaneous stabilization of multimachine power systems via genetic algorithms," *IEEE Trans. Power Syst.*, Vol. 14, pp. 1428–1437, November, 1999.
9. Abdel-Magic, Y. L., Abido, M. A., and Mantawy, A. H., "Robust tuning of power system stabilizer in multimachine power systems," *IEEE Trans. Power Syst.*, Vol. 15, pp. 735–740, May 2000.
10. Kenné, G., Gomab, R., Nkwawo, H., Lamnabhi-Lagarriague, F., Arzandé, A., and Vannier, J. C., "An improved direct feedback linearization technique for transient stability enhancement and voltage regulation of power generators," *Int. J. Elect. Power Energy Syst.*, Vol. 32, pp. 809–816, September 2010.
11. Ghoshal, S. P., Chatterjee, A., and Mukherjee, V., "Bio-inspired fuzzy logic based tuning of power system stabilize," *Expert Syst. Appl.*, Vol. 36, pp. 9281–9292, 2009.
12. El-Zonkoly, A. M., Khalil, A. A., and Ahmied, N. M., "Optimal tuning of lead-lag and fuzzy logic power system stabilizers using particle swarm optimization," *Expert Syst. Appl.*, Vol. 36, pp. 2097–2106, 2009.
13. Sebaaa, K., and Boudourb, M., "Optimal locations and tuning of robust power system stabilizer using genetic algorithms," *Elect. Power Syst. Res.*, Vol. 79, pp. 406–416, 2009.
14. Wang, S. K., Chiou, J. P., and Liu, C. W., "Parameters tuning of power system stabilizers using improved and direction hybrid differential evolution," *Elect. Power Energy Syst.*, Vol. 31, pp. 34–42, 2009.
15. Huerta, H., Loukianov, A. G., and Cañedo, J. M., "Decentralized sliding mode block control of multimachine power systems," *Int. J. Elect. Power Energy Syst.*, Vol. 32, pp. 1–11, January 2010.
16. Mitra, P., Chowdhury, S. P., Chowdhury, S., Pal, S. K., and Crossley, P. A., "Intelligent AVR and PSS with adaptive hybrid learning algorithm," *Proceedings of the PES General Meeting*, Pittsburgh, PA, 20–24 July 2008.
17. Corsi, S., "The secondary voltage regulation in Italy," *IEEE Summer Meeting*, Washington, 16–20 July 2000.
18. Brown, M., and C. Harris, "Adaptive B-spline networks," in *Neurofuzzy Adaptive Modelling and Control*, New York: Prentice Hall International, Chap. 8, 1994.
19. Saad, D., "Optimal on-line learning in multilayer neural networks," in *On-line Learning in Neural Networks*, UK: Cambridge University Press, Chap. 7, 1998.
20. Osman, A. H., Abdelazim, T., and Malik, O. P., "Transmission line distance relaying using on-line trained neural network," *IEEE Trans. on Power Delivery*, Vol. 20, No. 2, pp. 1257–1264, 2005.
21. Ramirez, J. M., Correa-Gutierrez, R. E., and Castrillon-Gutierrez, N. J., "A study on multiband PSS coordination," *Int. J. Emerging Elect. Power Syst.*, Vol. 10, No. 5, Article 6, 2009.
22. Castillo, I., Ramirez, J. M., and Tapia, R., "A genetic algorithm applied to enhance the damping of multi-machine power systems," *North American Power Symposium*, pp. 618–625, College Station, TX, 15–16 October 2001.
23. Padiyar, K. R., "Data for 10 generator system," in *Power System Dynamics: Stability & Control*, Singapore: John Wiley and Sons (Asia), 1996.
24. Chow, J. H., ed., "Reduced simulations of nonlinear power system models," in *Time-Scale Modeling of Dynamic Networks with Applications to Power Systems*, Germany: Springer, 1982.

Appendix

All data are in p.u. unless specified otherwise.

39-bus, 10-generator test system:

PSS data:

$$k = [435, 197, 593, 202, 212, 197, 535, 534, 267, 220];$$

$$T = 7.5;$$

$$T_1 = T_3 = 0.080;$$

$$T_2 = T_4 = 0.0150;$$

time constants have the same value for all machines.

SVR data:

$$\sigma = [0.1348, 0.1302, 0.125, 0.0968, 0.0499, 0.1862, 0.1194, 0.0123, 0.0355, 0.1098];$$

$$K_P = [1.3124, 2.4703, 1.3125, 2.6131, 1.3114, 2.4445, 1.0302, 2.4569, \\ 1.2720, 2.6140, 24.5029];$$

$$K_I = [1.0673, 0.0642, 1.9593, 1.0673, 0.0643, 1.9605, 1.0673, 0.0643, \\ 1.9603, 1.0673, 3.5711].$$

68-bus, 16-generator test system:

PSS data:

$$k = [372, 169, 508, 172, 182, 169, 458, 457, 228, 188, 85, 491, 506, 508, 211];$$

$$T = 7.5;$$

$$T_1 = T_3 = 0.080;$$

$$T_2 = T_4 = 0.0150;$$

time constants have the same value for all machines.

SVR data:

$$\sigma = [0.0413, 0.0660, 0.0711, 0.0383, 0.0581, 0.0786, 0.0353, 0.0001, 0.0018, \\ 0.0022, 0.0001, 0.0892, 0.3133, 0.0223, 0.0240, 0.1646];$$

$$K_P = [1.6276, 0.5611, 0.0700, 0.4856, 0.2472, 0.0700, 0.8305, 0.0700, 0.6148, \\ 0.7122, 0.0700, 5.8792, 0.0700, 1.2873, 0.0700, 2.3741, 0.0500];$$

$$K_I = [1.6265, 1.8538, 0.2613, 1.9473, 1.2986, 0.1832, 0.5770, 1.1292, 1.9500, \\ 1.9968, 0.3220, 2.0000, 0.0500, 1.9821, 1.0034, 1.6489, 1.0054].$$